Chapter 8
Performance Evaluation of Optical Noise-Impaired Multi-band OFDM Systems Through Analytical Modeling

Pedro E.D. Cruz, Tiago M.F. Alves and Adolfo V.T. Cartaxo

Abstract The performance evaluation through analytical modeling of virtual carrier-assisted direct-detection single-sideband multi-band orthogonal frequency division multiplexing (MB-OFDM) systems dominantly impaired by amplified spontaneous emission noise is presented. An analytical expression is obtained for the bit error ratio (BER) of these systems, using the analytical relationship between the electrical signal-to-noise ratio and the optical signal-to-noise ratio. In order to analyse the accuracy of the analytical expression, the BER estimates provided by the analytical model are compared with the ones obtained using numerical simulation and the exhaustive Gaussian approach. Excellent agreement between the BER estimates is verified when distortion does not affect significantly the performance of the MB-OFDM signal.

8.1 Introduction

Orthogonal frequency division multiplexing (OFDM) has been widely appointed as a powerful solution to provide capacity granularity and switching capabilities in optical networks [1–3]. Flexible bandwidth allocation was also identified as one of the main advantages of OFDM-based networks [4, 5]. Optical communication systems have also exploited the advantages of high spectral efficiency and resilience to linear fiber effects that OFDM can offer [4, 6]. Two different optical OFDM

P.E.D. Cruz (✉) · T.M.F. Alves · A.V.T. Cartaxo
Department of Electrical and Computer Engineering, Instituto Superior Técnico,
Optical Communications and Photonics Group, Instituto de Telecomunicações,
Universidade de Lisboa, Av. Rovisco Pais, 1, 1049-001 Lisbon, Portugal
e-mail: pedro.cruz@lx.it.pt

T.M.F. Alves
e-mail: tiago.alves@lx.it.pt

A.V.T. Cartaxo
e-mail: adolfo.cartaxo@lx.it.pt

flavors have been considered in the literature: (i) coherent-detection, where a local oscillator, hybrid couplers and several photodetectors are employed at the optical receiver, and (ii) direct-detection, where only one photodetector is required at the receiver. For systems where cost is of primary concern, such as in metropolitan networks, OFDM systems employing direct-detection are preferred [7].

Although optical OFDM systems have been widely studied, the implementation of multi-band OFDM (MB-OFDM) using direct-detection is a relatively new concept [8, 9]. A high-speed (>100 Gb/s) MB-OFDM system using a direct-detection optical OFDM superchannel (several OFDM bands) with dual carriers at both sides of the superchannel is proposed in [8] for long-haul networks. In that work, an analytical form to get the optimum carrier-to-signal power ratio is obtained in optical back-to-back, where only linear noise is considered. This kind of analytical formulation is of special interest as it allows obtaining a first estimate of system performance without requiring extensive numerical simulations to acquire the results. Although the system presented in [8] has high spectral efficiency, it is quite challenging to implement this MB-OFDM system in flexible metropolitan networks mainly due to huge requirements for the receiver front-end bandwidth. The optical OFDM superchannel proposed in [9], which is a variant of the MB-OFDM direct-detection long-haul system of [8], proposes the use of multiple carriers along the superchannel. In [9], a carrier supports a few OFDM bands, targeting ultra-high capacity with more relaxed receiver front-end bandwidth requirements, when comparing with the system of [8]. These two MB-OFDM systems [8, 9] have proposed and demonstrated effective direct-detection solutions for long-haul networks. This paper considers a different MB-OFDM system, where one carrier supports one OFDM band. In this system, the pair OFDM band-carrier is selected by optical filtering before direct detection, reducing the required bandwidth of the front-end receiver significantly, when comparing with the receiver bandwidth requirements of the systems presented in [8, 9]. This MB-OFDM system presents some challenges that require investigation, such as the crosstalk originated by the finite selectivity of the optical filters or the effect of increasing the spectral efficiency by reducing the gap between the carrier and the OFDM band on the system performance.

In this work, the performance of an amplified spontaneous emission (ASE) noise-impaired direct-detection single-sideband (SSB) MB-OFDM system employing a virtual carrier per OFDM signal is analytically modeled, by using the bit error ratio (BER) as figure of merit. Operation in optical back-to-back is considered, as optical fiber impairments should not present remarkable influence on the performance of SSB systems.

8.2 System Description

The model considered to describe the MB-OFDM system in optical back-to-back is presented in Fig. 8.1.
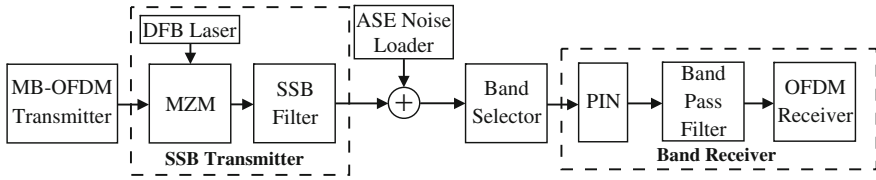
Fig. 8.1 MB-OFDM system model in optical back-to-back. *ASE* amplified spontaneous emission; *DFB* distributed feedback; *MZM* Mach-Zehnder modulator; *PIN* positive-intrinsic-negative; *SSB* single-sideband

The radiofrequency (RF) MB-OFDM signal generated at the MB-OFDM transmitter is composed by N_B OFDM signals (or bands) and N_B RF carriers (or virtual carriers—VCs), as depicted in Fig. 8.2.

The MB-OFDM system considers one VC per OFDM band. Each pair band-VC does not interfere in frequency with the corresponding neighboring pairs. The virtual-carrier-to-band gap (VBG) is selected in order to avoid the signal-signal beat interference (SSBI) originated by the photodetector square-law. A MB-OFDM system design with the VC at a higher frequency than the corresponding OFDM band is considered. At the SSB transmitter, the optical signal is generated by a distributed feedback (DFB) laser and the MB-OFDM signal modulates that optical signal using a chirpless Mach-Zehnder modulator (MZM), biased at quadrature point. The optical signal at the MZM output is then filtered by a SSB filter, creating a SSB signal. This allows overcoming the chromatic dispersion-induced power fading impairment caused by the square-law photodetection of a double-sided optical signal transmitted along a dispersive medium. After SSB filtering, an ASE noise loader adds optical noise to the MB-OFDM signal. After ASE noise addition, the band and VC to be dropped at the receiver are selected by the band selector (BS) optical filter. The band receiver is composed by a positive-intrinsic-negative (PIN) photodetector, a band pass filter (BPF) and an OFDM receiver. The PIN converts the optical signal to an electrical signal. The BPF removes the out-of-band noise and filters the received OFDM signal, and the OFDM receiver digitally-converts and demodulates the electrical signal.
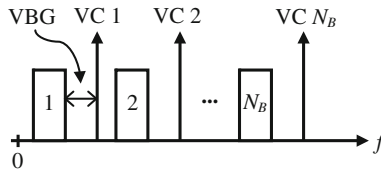

Fig. 8.2 Simplified scheme of a MB-OFDM signal, with N_B bands and N_B VCs. *VBG* virtual-carrier-to-band gap

8.3   Analytical Modeling

In this section, the analytical modeling of the signal and noise power along the MB-OFDM system is performed. The main objective is to obtain analytical expressions for the optical signal-to-noise ratio (OSNR) and the electrical signal-to-noise ratio (ESNR) at the BPF output. With these expressions, fast BER estimates can be obtained to provide insight on the performance of SSB MB-OFDM systems employing direct-detection.

The RF signal at the MZM input, $v_{RF}(t)$, can be written as:

$$v_{RF}(t) = \underbrace{[s_b(t) + A_v s_v(t)]}_{s_e(t)} \frac{V_{RMS,imp}}{V_{RMS,s_e(t)}},$$ (8.1)

with

$$s_b(t) = \sum_{n=1}^{N_B} \frac{s_{b,n}(t)}{V_{RMS,s_{b,n}(t)}},$$ (8.2)

and

$$s_v(t) = \sum_{n=1}^{N_B} \frac{s_{v,n}(t)}{V_{RMS,s_{v,n}(t)}},$$ (8.3)

where $s_b(t)$ is the sum of all up-converted N_B OFDM band signals, A_v is the amplitude of each VC, $s_v(t)$ is the sum of all N_B VCs, $s_{b,n}(t)$ is the nth OFDM band, $V_{RMS,s_{b,n}(t)}$ is the root-mean-square (RMS) voltage of $s_{b,n}(t)$, $s_{v,n}(t)$ is the nth VC, $V_{RMS,s_{v,n}(t)}$ is the RMS voltage of $s_{v,n}(t)$, $s_e(t)$ is the MB-OFDM signal, $V_{RMS,s_e(t)}$ is the RMS voltage of $s_e(t)$, and $V_{RMS,imp}$ is the RMS voltage imposed to the MB-OFDM signal at the MZM input. As a note, $v_{RF}(t)$ can be written as:

$$v_{RF}(t) = s_{b,e}(t) + s_{v,e}(t),$$ (8.4)

with

$$\begin{cases} s_{b,e}(t) = \frac{V_{RMS,imp}}{V_{RMS,s_e(t)}} s_b(t), \\ s_{v,e}(t) = \frac{V_{RMS,imp} A_v}{V_{RMS,s_e(t)}} s_v(t), \end{cases}$$ (8.5)

and the mean power of $v_{RF}(t)$, p_{RF}, is given by:

$$p_{RF} = V_{RMS,imp}^2.$$ (8.6)

The output electrical field of a chirpless MZM, $e_{MZM}(t)$, can be expressed as:

$$e_{MZM}(t) = E_i \cos\left\{\frac{\pi}{2V_\pi}[-V_b + v_{RF}(t)]\right\} \exp(j2\pi v_0 t), \qquad (8.7)$$

where E_i is the optical field at the MZM input, V_b is the MZM bias voltage, V_π is the voltage required to switch between the maximum and the minimum of the MZM power transmission characteristic, and v_0 is the optical frequency.

Considering a linearized MZM by applying the Taylor series first-order approximation around zero with respect to $v_{RF}(t)$, and that the MZM is biased at quadrature point ($V_b = V_\pi/2$), the linearized output field, $e_{MZM,l}(t)$, can be written as:

$$e_{MZM,l}(t) = E_i \left[\frac{\sqrt{2}}{2} + \frac{\sqrt{2}}{4}\frac{\pi}{V_\pi} v_{RF}(t)\right] \exp(j2\pi v_0 t). \qquad (8.8)$$

Using (8.4) and (8.5), and knowing that:

$$\begin{cases} \left\langle |s_b(t)|^2 \right\rangle = \left\langle |s_v(t)|^2 \right\rangle = N_B, \\ V^2_{RMS,s_e(t)} = N_B(1 + A_v^2), \end{cases} \qquad (8.9)$$

the mean power at the linearized MZM output, $p_{MZM,l}$, can be expressed as:

$$p_{MZM,l} = \underbrace{\frac{E_i^2}{2}}_{p_o} + \underbrace{\frac{1}{8}\frac{\pi^2}{V_\pi^2}E_i^2\frac{V^2_{RMS,imp}}{1 + A_v^2}}_{p_b} + \underbrace{\frac{1}{8}\frac{\pi^2}{V_\pi^2}E_i^2\frac{V^2_{RMS,imp}}{1 + A_v^2}A_v^2}_{p_v}, \qquad (8.10)$$

where p_0 is the optical carrier mean power, p_v is the mean power of all the VCs, and p_b is the mean power of all the OFDM bands.

Two important power ratios can be determined from (8.10), which are the virtual-carrier-to-band power ratio (VBPR) and the optical-carrier-to-band power ratio (OBPR). These ratios are important because they have a significant impact on the performance of the MB-OFDM signal. The VBPR is given by:

$$\text{VBPR} = \frac{p_v}{p_b} = \frac{p_{v,n}}{p_{b,n}} = A_v^2, \qquad (8.11)$$

and the OBPR can be written as:

$$\text{OBPR} = \frac{p_o}{p_b} = \frac{4V_\pi^2(1 + \text{VBPR})}{\pi^2 V^2_{RMS,imp}}, \qquad (8.12)$$

where $p_{v,n} = p_v/N_B$ and $p_{b,n} = p_b/N_B$ are the mean power of the VCn and the OFDM band n, respectively.

After electro-optical conversion, SSB filtering is performed and the lower sideband and lower VC are removed. After some calculations, the mean power at the SSB filter output, p_{SSB}, can be expressed as:

$$p_{SSB} = p_o + \frac{p_v}{2} + \frac{p_b}{2}. \tag{8.13}$$

Afterwards, an ASE noise loader is added to the signal at the SSB filter output. Hence, it is important to define the OSNR after noise loading (NL).

Considering that the ASE noise is zero-mean additive-white-Gaussian and is present in the parallel ($\parallel$) and perpendicular ($\perp$) polarization directions, and that the signal field at the SSB filter output is polarized in the parallel direction, the low pass equivalent (LPE) of the field after NL, $\mathbf{e}_{NL}(t)$, can be expressed as:

$$\mathbf{e}_{NL}(t) = \left[e_{SSB,\parallel}(t) + n_{I,\parallel}(t) + j\,n_{Q,\parallel}(t) \right]\mathbf{u}_{\parallel} + \left[n_{I,\perp}(t) + j\,n_{Q,\perp}(t) \right]\mathbf{u}_{\perp}, \tag{8.14}$$

where $e_{SSB,\parallel}(t)$ is the OFDM signal field at the SSB filter output in the $\parallel$ polarization defined by $\mathbf{u}_{\parallel}$, $n_{I,\parallel}(t)$ and $n_{Q,\parallel}(t)$ are the I and Q noise components in the $\parallel$ polarization, respectively, and $n_{I,\perp}(t)$ and $n_{Q,\perp}(t)$ are the I and Q noise components in the $\perp$ polarization defined by $\mathbf{u}_{\perp}$, respectively.

Assuming that each one of the four noise components has a constant power spectral density (PSD) given by S_{ASE}, the optical noise mean power in a bandwidth B_N after NL, $p_{n,NL}$, can be expressed as:

$$p_{n,NL} = 4 S_{ASE} B_N. \tag{8.15}$$

Usually, B_N corresponds to a reference bandwidth of 0.1 nm, which is approximately 12.5 GHz.

The OSNR is defined as the ratio between the signal power after NL, $p_{s,NL}$ (which is equal to the signal power at the SSB filter output, p_{SSB}), and the noise mean power, $p_{n,NL}$, in the reference bandwidth B_N, after NL. Considering (8.13) and (8.15), the OSNR is then expressed as:

$$\text{OSNR} = \frac{p_{s,NL}}{p_{n,NL}} = \frac{p_{SSB}}{p_{n,NL}} = \frac{p_o + \frac{p_v}{2} + \frac{p_b}{2}}{4 S_{ASE} B_N}. \tag{8.16}$$

After ASE noise loading, the BS is used to select the OFDM band and VC that will be photodetected (dropped). The BS is an ideal optical filter, with transfer function $H_{BS,n}(f)$ and impulse response $h_{BS,n}(t)$, that only selects the nth OFDM signal and the nth VC. The LPE of $H_{BS,n}(f)$ can be written as:

$$H_{BS,n}(f) = \text{rect}\left(\frac{f - f_x}{B_o} \right), \tag{8.17}$$

where B_0 is the BS bandwidth and f_x is the center frequency of the BS given by:

$$f_x = \frac{f_{\max} + f_{\min}}{2} = \frac{f_{v,n} + \left(f_{RF,n} - \frac{B_E}{2}\right)}{2},\tag{8.18}$$

where $f_{v,n}$ is the nth VC frequency, $f_{RF,n}$ is the nth band central frequency, $f_{\max}$ and $f_{\min}$ are the maximum and minimum frequencies of the passband of the BS, respectively, and B_E is the OFDM signal bandwidth.

The LPE of the signal at the BS output, $\mathbf{e}_{BS,n}(t)$, can be expressed as:

$$\begin{aligned}
\mathbf{e}_{BS,n}(t) &= \mathbf{e}_{NL}(t) \circledast h_{BS,n}(t) \\
&= \left[\mathbf{e}_{BS,n,\|}(t) + n'_{I,\|}(t) + jn'_{Q,\|}(t) \right] \mathbf{u}_\| + [n'_{I,\perp}(t) + jn'_{Q,\perp}(t)] \mathbf{u}_\perp,
\end{aligned}\tag{8.19}$$

where $\circledast$ denotes the convolution operation, $e_{BS,n,\|}(t)$ is the field, at the BS output, of the nth OFDM signal and nth VC in the $\|$ polarization, $n'_{I,\|}(t)$ and $n'_{Q,\|}(t)$ are the filtered I and Q noise components in the $\|$ polarization, respectively, and $n'_{I,\perp}(t)$ and $n'_{Q,\perp}(t)$ are the filtered I and Q noise components in the $\perp$ polarization, respectively. The field $e_{BS,n,\|}(t)$ is given by:

$$\begin{aligned}
e_{BS,n,\|}(t) = \frac{\sqrt{2}}{4} \frac{\pi}{V_\pi} E_i &\left[\frac{V_{RMS,imp}}{V_{RMS,s_e(t)} V_{RMS,s_{b,n}(t)}} s_{b,n}(t) \right. \\
&\left. + \frac{V_{RMS,imp} A_v}{V_{RMS,s_e(t)} V_{RMS,s_{v,n}(t)}} s_{v,n}(t) \right] \exp(j2\pi v_0 t),
\end{aligned}\tag{8.20}$$

with

$$s_{b,n}(t) = s_{I,n}(t) \cos(2\pi f_{RF,n} t) - s_{Q,n}(t) \sin(2\pi f_{RF,n} t),\tag{8.21}$$

and

$$s_{v,n}(t) = \sqrt{2} \cos(2\pi f_{v,n} t + \phi_v),\tag{8.22}$$

where $s_{I,n}(t)$ is the low pass in-phase (I) component of the OFDM signal of band n, $s_{Q,n}(t)$ is the low pass quadrature (Q) component of the OFDM signal of band n, and ϕ_v is the VC initial phase.

The field $e_{BS,n,\|}(t)$ has a mean power, $p_{BS,n}$, given as follows:

$$p_{BS,n} = \frac{p_v + p_b}{2N_B} = \frac{p_{v,n}}{2} + \frac{p_{b,n}}{2}.\tag{8.23}$$

After band selection, the signal is photodetected. The PIN model used in this work is a square modulus function with responsivity R_λ of 1 A/W. The photocurrent at the PIN output, $i_{PIN,n}(t)$, can be written as:

$$i_{PIN,n}(t) = |\mathbf{e}_{BS,n}(t)|^2 = \left|e_{BS,n,\|}(t) + n'_{I,\|}(t) + jn'_{Q,\|}(t)\right|^2 + |n'_{I,\perp}(t) + jn'_{Q,\perp}(t)|^2. \tag{8.24}$$

After some calculations, the PIN output current can be separated in two groups: the signal-dependent current and the noise-dependent current. The signal dependent current, denoted as $i_{s,PIN}(t)$, is given by:

$$
\begin{aligned}
i_{s,PIN}(t) = \frac{1}{8}\frac{\pi^2}{V_\pi^2}E_i^2 \times & \left[\frac{1}{4}\left(\frac{V_{RMS,imp}}{V_{RMS,s_{b,n}(t)}V_{RMS,s_e(t)}}\right)^2 \left[s_{I,n}^2(t) + s_{Q,n}^2(t)\right] \right. \\
& + \frac{\sqrt{2}}{2}\frac{V_{RMS,imp}^2 A_\upsilon}{V_{RMS,s_{b,n}(t)}V_{RMS,s_{\upsilon,n}(t)}V_{RMS,s_e(t)}^2}s_{PIN}(t) \\
& \left. + \frac{1}{2}\left(\frac{V_{RMS,imp}A_\upsilon}{V_{RMS,s_{\upsilon,n}(t)}V_{RMS,s_e(t)}}\right)^2 \right],
\end{aligned}
\tag{8.25}
$$

with

$$s_{PIN}(t) = s_{I,n}(t)\cos\left[2\pi\big(f_{\upsilon,n} - f_{RF,n}\big)t\right] + s_{Q,n}(t)\sin\left[2\pi\big(f_{\upsilon,n} - f_{RF,n}\big)t\right]. \tag{8.26}$$

The first term of $i_{s,PIN}(t)$ is the SSBI, the second term is the received OFDM signal, and the third term is the direct-current (DC) component. The Fourier transform of $i_{s,PIN}(t)$, $I_{s,PIN}(f)$, is given by:

$$
\begin{aligned}
I_{s,PIN}(f) = \frac{1}{8}\frac{\pi^2}{V_\pi^2}E_i^2 \times & \left[\frac{1}{4}\left(\frac{V_{RMS,imp}}{V_{RMS,s_{b,n}(t)}V_{RMS,s_e(t)}}\right)^2 S_d(f) \right. \\
& + \frac{\sqrt{2}}{2}\frac{V_{RMS,imp}^2 A_\upsilon}{V_{RMS,s_{b,n}(t)}V_{RMS,s_{\upsilon,n}(t)}V_{RMS,s_e(t)}^2}S_{PIN}(f) \\
& \left. + \frac{1}{2}\left(\frac{V_{RMS,imp}A_\upsilon}{V_{RMS,s_{\upsilon,n}(t)}V_{RMS,s_e(t)}}\right)^2 \delta(f) \right],
\end{aligned}
\tag{8.27}
$$

with $S_d(f) = \mathscr{F}\{s_{I,n}^2(t) + s_{Q,n}^2(t)\}$ and $S_{PIN}(f) = \mathscr{F}\{s_{PIN}(t)\}$, where $\mathscr{F}\{\cdot\}$ denotes the Fourier transform. The noise-dependent current, denoted as $i_{n,PIN}(t)$, where the noise-noise beat terms were neglected, can be expressed as:

$$i_{n,PIN}(t) = e_{BS,n,\|}(t)\left[n'_{I,\|}(t) - jn'_{Q,\|}(t)\right] + \left\{e_{BS,n,\|}(t)\left[n'_{I,\|}(t) - jn'_{Q,\|}(t)\right]\right\}^*. \tag{8.28}$$

In order to obtain the noise PSD at the PIN output, $S_{n,PIN}(f)$, the Fourier transform of the auto-correlation function of $i_{n,PIN}(t)$ must be evaluated. After performing some calculations, $S_{n,PIN}(f)$ is given by:

$$S_{n,PIN}(f) = 2S_{ASE}\left[\left|H_{BS,n}(f+f_{v,n})\right|^2 + \left|H_{BS,n}(-f+f_{v,n})\right|^2\right]p_{BS,n}. \quad (8.29)$$

After photodetection, a BPF is used to remove the SSBI and the DC component from the photodetected signal. The BPF transfer function, $H_{BPF}(f)$, is given by:

$$H_{BPF}(f) = \text{rect}\left(\frac{f - f_{RF,n} + f_{v,n}}{B_E}\right) + \text{rect}\left(\frac{f + f_{RF,n} - f_{v,n}}{B_E}\right), \quad (8.30)$$

where B_E is the BPF bandwidth, which is equal to the OFDM signal bandwidth. The Fourier transform, $I_{s,BPF}(f)$, of the signal at the BPF output, can be expressed as:

$$I_{s,BPF}(f) = I_{s,PIN}(f)H_{BPF}(f), \quad (8.31)$$

which is approximately given by:

$$I_{s,BPF}(f) \approx \frac{1}{8}\frac{\pi^2}{V_\pi^2}E_i^2\frac{\sqrt{2}}{2} \times \frac{V_{RMS,imp}^2 A_v}{V_{RMS,s_{b,n}(t)} V_{RMS,s_{v,n}(t)} V_{RMS,s_e(t)}^2}S_{PIN}(f)H_{BPF}(f). \quad (8.32)$$

After some calculations, the mean power of $I_{s,BPF}(f)$, $p_{s,BPF}$, can be written as:

$$p_{s,BPF} = \frac{p_{v,n}p_{b,n}}{2}. \quad (8.33)$$

The noise power at the BPF output can be obtained from the PSD of the noise at the PIN output (8.29) as:

$$p_{n,BPF} = \int_{-\infty}^{+\infty} S_{n,PIN}(f)|H_{BPF}(f)|^2\,\mathrm{d}f = 4p_{BS,n}S_{ASE}B_E, \quad (8.34)$$

where B_E is the bandwidth of the low pass filter at the receiver (which has the greatest frequency limitation). The ESNR is defined as the ratio between the signal power, $p_{s,BPF}$, and the noise mean power, $p_{n,BPF}$, at the BPF output. Considering (8.33) and (8.34), the ESNR is then given by:

$$\text{ESNR} = \frac{p_{s,BPF}}{p_{n,BPF}} = \frac{\frac{p_{v,n}p_{b,n}}{2}}{\left(\frac{p_{v,n}+p_{b,n}}{2}\right)4S_{ASE}B_E}. \quad (8.35)$$

8.4 Performance Evaluation Metric

Figure of merit used in this study to categorize the system performance is the BER, which can be estimated as a function of the ESNR with the following expression [8]:

$$\text{BER} = \frac{1 - \frac{1}{\sqrt{M}}}{\log_2(\sqrt{M})} \text{erfc}\left(\sqrt{\frac{3\,\text{ESNR}\,\log_2(\sqrt{M})}{(M-1)\log_2(M)}}\right), \qquad (8.36)$$

where erfc($\cdot$) is the complementary error function, and M is the number of distinct symbols of the quadrature amplitude modulation format. Knowing that $p_o/p_{b,n} = N_B \times \text{OBPR}$, $p_v/p_{b,n} = N_B \times \text{VBPR}$, $p_b/p_{b,n} = N_B$, and using (8.35) and (8.16), the ESNR can be expressed as:

$$\text{ESNR} = \frac{1}{N_B}\frac{2}{(2 \times \text{OBPR} + \text{VBPR} + 1)}\frac{\text{VBPR}}{(\text{VBPR} + 1)}\frac{B_N}{B_E}\text{OSNR}. \qquad (8.37)$$

Some important conclusions can be derived from (8.37). Keeping OBPR and VBPR constant, the ESNR of one band is inversely proportional to N_B, which means that transmitting more than one band will require an OSNR increase proportional to the number of bands to achieve the same performance as when only one band is transmitted. An increase of VBPR (that also results in an OBPR increase, as the OBPR depends on the VBPR) will also lead to a higher required OSNR, to achieve the same performance obtained with low VBPR. The power attributed to the OFDM band decreases and the power assigned to the VC increases, meaning lower ESNR.

8.5 Numerical Results

The effectiveness of the proposed analytical model for MB-OFDM systems is assessed by comparing its estimates with the ones of numerical simulation using MATLAB. The OSNR that leads to a BER = 10^{-3} (OSNR$_{req}$) and the BER itself are used as figures of merit. To assess the analytical method (AM) accuracy, the BER obtained with the AM is compared with the BER retrieved from numerical simulation (NS) using the exhaustive Gaussian approach (EGA) [10]. In the analysis, each OFDM symbol has 128 subcarriers, each OFDM band has a bit rate of 5 Gb/s and a bandwidth of 2.5 GHz, the maximum total bit rate (assuming a maximum of 4 bands) is 20 Gb/s, and the following parameters are fixed: $M = 4$, $V_\pi = 5$V, $B_E = 2.5$ GHz, $B_N = 12.5$ GHz, GHz, $f_{RF,n} \in$ [2.25, 8.25, 14.25, 20.25] GHz and $f_{v,n}$ [6, 12, 18, 24] GHz with $n \in$ [1–4].

The linearized MZM with the relationship between the applied voltage and field at the MZM output given by (8.8) is used in the numerical results. A particular

study, in which a real MZM is considered in the simulation, is also performed and explicitly mentioned. The target of this particular study is to assess the validity range of the AM in presence of MZM distortion. With the real MZM, is important to impose that the VC frequencies are multiple of $f_{v,1}$ (in this work, $f_{v,1} = 6$ GHz), in order to guarantee that the inter-modulation products of the VCs do not interfere with the OFDM bands.

The number of bands affects significantly the performance of the MB-OFDM system, as it was concluded through analysis of (8.37). Figure 8.3 shows the $OSNR_{req}$ as function of $V_{RMS,imp}$ for $N_B = [1, 2, 4]$, obtained with the AM and with NS. A VBPR of 15 dB is imposed. Figure 8.3 shows that the AM results have excellent agreement with the ones obtained with NS. Figure 8.3 also demonstrates that when N_B doubles, the $OSNR_{req}$ increases 3 dB. Figure 8.3 shows also that increasing $V_{RMS,imp}$ leads to a $OSNR_{req}$ decrease, which is valid for this system because it does not exhibit MZM distortion.

Another parameter besides N_B that influence significantly the performance results is the VBPR. Figure 8.4 shows the $OSNR_{req}$ as function of $V_{RMS,imp}$ for VBPR = [3, 9, 15] dB, with the AM and with NS. The MB-OFDM system has four bands ($N_B = 4$). Figure 8.4 shows an excellent agreement between the AM results and the NS results. Figure 8.4 also shows that increasing VBPR leads to an increase of the $OSNR_{req}$. This increase is higher for higher VBPRs.

In the results of Figs. 8.3 and 8.4, the VBG is selected in order to avoid the SSBI overlapping with the received OFDM band. However, it is important to verify the resilience of the AM when PIN distortion interferes with the information-bearing signal, as a smaller VBG means more spectral efficiency. Figure 8.5 shows the BER as function of the VBG width in GHz, for VBPR = [3, 9, 15] dB and $V_{RMS,imp} = 1500$ mV. The OSNR is 22.4 dB for VBPR = 3 dB, 25.9 dB for VBPR = 9 dB and 31.1 dB for VBPR = 15 dB. With these OSNR levels and as the AM does not take into account the PIN distortion, the BER obtained using the AM is 10^{-3} for all VBG widths. Therefore, Fig. 8.5 only shows the NS results.

Fig. 8.3 $OSNR_{req}$ as function of $V_{RMS,imp}$ for $N_B = [1, 2, 4]$, with AM (*solid lines*) and NS (*dashed lines*), with a fixed VBPR of 15 dB
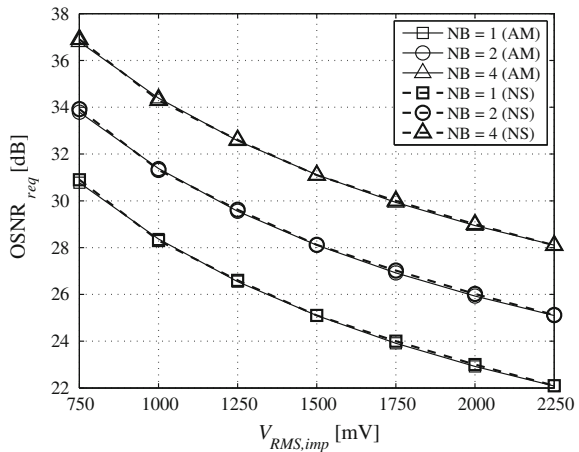
Fig. 8.4 OSNR$_{req}$ as function of $V_{RMS,imp}$ for VBPR = [3, 9, 15] dB, with AM (*solid lines*) and NS (*dashed lines*), and with $N_B = 4$
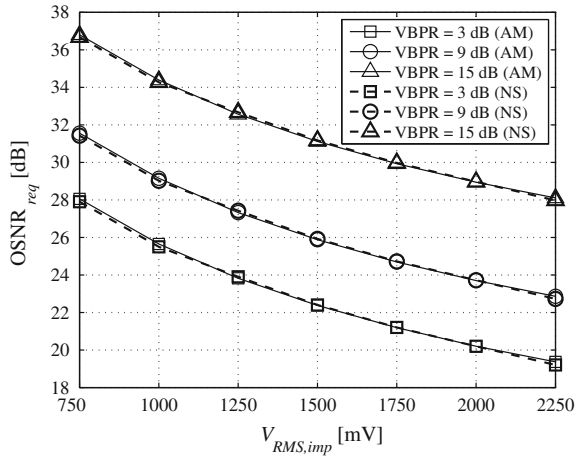

Figure 8.5 shows that the SSBI caused by the PIN affects the performance when the VBG width is lower than the bandwidth of the OFDM signal, as the SSBI spectrum overlaps the OFDM signal spectrum. Figure 8.5 shows also that the BER degrades more substantially for lower VBPRs. This is because lower VBPR levels leads to more SSBI power.

The results shown in Figs. 8.3, 8.4 and 8.5 present the effects of ASE noise and PIN distortion on the performance. However, the effects of MZM distortion were not considered in the simulation in those results as a linearized MZM is assumed in the analytical formulation. To illustrate the impact of MZM nonlinearity on the required OSNR and assess the validity range of the AM presented in this work, a real MZM described by (8.7) is considered in the simulation.

Figure 8.6 shows the OSNR$_{req}$ as function of the $V_{RMS,imp}$, for VBPR = [3, 9, 15] dB, and for the first band which is the most affected by MZM distortion. The

Fig. 8.5 BER as function of the VBG width, for VBPR = [3, 9, 15] dB and $V_{RMS,imp} = 1500$ mV, with NS. With the AM, the BER is 10^{-3} for all VBG widths
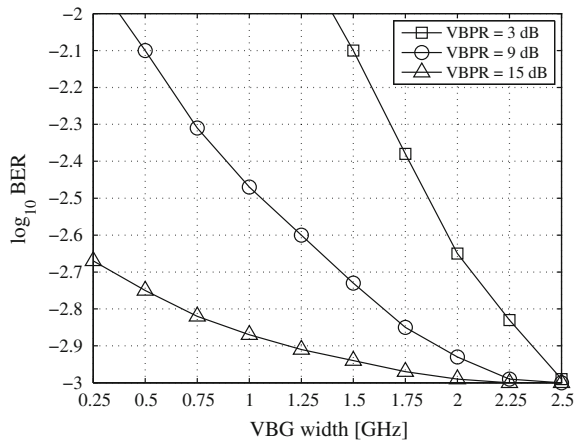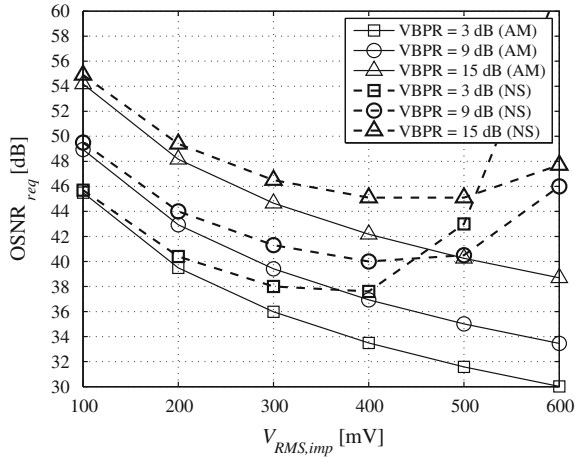
Fig. 8.6 OSNR$_{req}$ as function
of the $V_{RMS,imp}$, for
VBPR = [3, 9, 15] dB.
A MB-OFDM system with 4
bands ($N_B = 4$) is considered.
A real MZM is considered in
the simulation

MB-OFDM system has four bands ($N_B = 4$), and a VBG width of 2.5 GHz is imposed. Figure 8.6 shows that the MZM distortion causes a performance degradation as the RMS voltage increases. For RMS voltages around 400 mV, the minimum OSNR$_{req}$ is obtained. From the simulation results, the minimum OSNR$_{req}$ for VBPR = 3 dB is 38 dB, for VBPR = 9 dB is 40 dB, and for VBPR = 15 dB is 45 dB. The error committed by the AM in the minimum OSNR$_{req}$ is approximately 4 dB for VBPR = 3 dB and for VBPR = [9, 15] dB is approximately 3 dB. The analytical modeling of this work assumes noise-impaired MB-OFDM systems. Hence distortion-impaired systems are not well described by this model. This occurs for $V_{RMS,imp}$ higher than approximately 200 mV, which in modulation index ($V_{RMS,imp}/V_{\pi}$ in percentage) is 4 %.

8.6   Conclusions

An analytical model for performance evaluation of ASE noise-impaired direct-detection SSB MB-OFDM systems has been proposed. The effectiveness of the analytical model has been verified through comparison with numerical simulation using the EGA to evaluate the BER. Excellent agreement in the BER results when MZM and PIN distortion do not interfere with the MB-OFDM signal has been shown. When PIN distortion is affecting the MB-OFDM signal, the analytical model provides more accurate estimates for high VBPRs. When MZM distortion is interfering with the MB-OFDM signal, the analytical model presents a deviation in the required OSNR not exceeding 1 dB, for modulation indexes lower than 4 %. The analytical modeling for distortion-impaired MB-OFDM systems, as well as the MB-OFDM system optimization in order to achieve the best required OSNR, will be reported elsewhere.

References

1. N. Cvijetic, OFDM for next-generation optical access networks. J. Lightw. Technol. **30**, 384–398 (2012)
2. S. Blouza, J. Karaki, N. Brochier, E. Rouzic, E. Pincemin, B. Cousin, Multi-band OFDM for optical networking, Paper presented at the Int. Conf. Comput. Tool. doi:10.1109/EUROCON.2011.5929191
3. K. Christodoulopoulos, I. Tomkos, E. Varvarigos, Elastic bandwidth allocation in flexible OFDM-based optical networks. J. Lightw. Technol. **29**, 1354–1366 (2011)
4. J. Armstrong, OFDM for optical communications. J. Lightw. Technol. **27**, 189–204 (2009)
5. W. Shieh, OFDM for flexible high-speed optical networks. J. Lightw. Technol. **29**, 1560–1577 (2011)
6. A. Lowery, L. Du, J. Armstrong, Orthogonal frequency division multiplexing for adaptive dispersion compensation in long haul WDM systems. Paper presented at the Opt. Fiber Commun. Conf., paper PDF39 (2006)
7. S. Kim, K. Seo, J. Lee, Spectral efficiencies of channel-interleaved bidirectional and unidirectional ultradense WDM for metro applications. J. Lightw. Technol. **30**, 229–233 (2012)
8. W. Peng, I. Morita, H. Takahashi, T. Tsuritani, Transmission of high-speed (>100 Gb/s) direct-detection optical OFDM superchannel. J. Lightw. Technol. **30**, 2025–2034 (2012)
9. Z. Li, X. Xiao, T. Gui, Q. Yang, R. Hu, Z. He, M. Luo, C. Li, X. Zhang, D. Xue, S. You, S. Yu, 432-Gb/s direct-detection optical OFDM superchannel transmission over 3040-km SSMF. IEEE Photon. Technol. Lett. **25**, 1524–1526 (2013)
10. T. Alves, A. Cartaxo, Extension of the exhaustive Gaussian approach for BER estimation in experimental direct-detection OFDM setups. Microw. Opt. Technol. Lett. **52**, 2772–2775 (2010)